Dynamic Morphometrics Reveals Contributions of Dendritic Growth Cones and Filopodia to Dendritogenesis in the Intact and Awake Embryonic Brain

Sharmin Hossain, D. Sesath Hewapathirane, Kurt Haas

Department of Cellular and Physiological Sciences, Program in Neuroscience, Brain Research Centre, University of British Columbia, Vancouver V6T2B5, BC, Canada

Received 22 May 2011; revised 17 July 2011; accepted 21 July 2011

ABSTRACT: **Using *in vivo* rapid and long-interval two-photon time-lapse imaging of brain neuronal growth within the intact and unanesthetized *Xenopus laevis* tadpole, we characterize dynamic dendritic growth behaviors of filopodia, branches, and dendritic growth cones (DGCs), and analyze their contribution to persistent arbor morphology. The maturational progression of dynamic dendritogenesis was captured by short-term, 5 min interval, imaging for 1 h every day for 5 days, and the contribution of short-term growth to persistent structure was captured by imaging at 5 min intervals for 5 h, and at 2 h intervals for 10 h during the height of arbor growth. We find that filopodia and branch stability increases with neuronal maturation, and while the majority of dendritic filopodia rapidly retract, 3% to 7% of interstitial filopodia transition into persistent branches with lifetimes greater than 90 min. Here, we provide the first characterization of DGC dynamics, including morphology and behavior, in the intact and awake developing vertebrate brain. We find that DGCs occur on all growing branches indicating an essential role in branch elongation, and that DGC morphology correlates with dendritic branch growth behavior and varies with maturation. These results demonstrate that dendritogenesis involves a remarkable amount of continuous remodeling, with distinct roles for filopodia and DGCs across neuronal maturation.** © 2011 Wiley Periodicals, Inc. Develop Neurobiol 72: 615–627, 2012

***Keywords: Xenopus laevis*; tadpole; two-photon microscopy; *in vivo* imaging; development; dendritogenesis; dendritic growth cone; filopodia**

INTRODUCTION

The structural development of brain circuits is one of the most complex processes in early life critical to future brain function and is susceptible to errors that may give rise to neurodevelopmental disorders. Brain neurons must grow elaborate dendritic and axonal arbors and form precise inter-neuronal synaptic connections to create the physical structure necessary for functional neural circuits. Establishing correct dendritic arbor morphologies is required to contact appropriate axons, to provide surface area for synaptic inputs, and to influence electrical properties underlying the integration, processing, and plasticity of synaptic currents (Hausser et al., 2000). The mechanisms regulating neuronal dendritic arbor growth are beginning to emerge, and involve a combination of intrinsic genetic programming to establish basic neuron-type specific patterning and extrinsic cues that underlie individual neuronal variations, as well as extensive activity-dependent remodeling (McAllister et al., 1997, Nedivi et al., 1998, Rajan and Cline, 1998, Wu

Correspondence to: K. Haas (kurt.haas@ubc.ca).

Published online 26 July 2011 in Wiley Online Library (wileyonlinelibray.com).
DOI 10.1002/dneu.20959

et al., 1999, Polleux et al., 2000, Sin et al., 2002, Grueber et al., 2003, Haas et al., 2006, Jinushi-Nakao et al., 2007, Jan and Jan, 2010).

Our understanding of mechanisms underlying dendritogenesis has been greatly advanced by the recent development of technologies allowing direct imaging of neuronal growth within intact developing brains. *In vivo* rapid time-lapse imaging of individual growing brain neurons in transparent embryos of albino *Xenopus laevis* tadpoles and zebrafish has provided new insights to how growing dendritic arbors achieve their mature shapes (Wu et al., 1999, Niell et al., 2004, Mumm et al., 2006, Liu et al., 2009, Chen et al., 2010). Sampling entire growing dendritic arbors at intervals of minutes, over periods of hours, reveals an exceptional amount of motility and turnover of both short filopodia and longer branches, which could not be predicted from imaging at longer intervals. Another feature of growth readily apparent from rapid time-lapse imaging is the high incidence of dendritic growth cones (DGCs) at the tips of branches, which are often not evident in single time point images because of their highly variable morphologies with sparse expression of lamellipodia. High interstitial filopodial turnover and the presence of dynamic DGCs suggest mechanisms by which extrinsic factors, such as presynaptic input, growth factors and guidance cues may influence dendritic arbor patterning.

While interstitial dendritic filopodia are largely associated with spine formation in neurons with established dendritic arbors, it has been postulated that in immature growing neurons, they are precursors of longer branches (Dailey and Smith, 1996, Wu et al., 1999, Scott and Luo, 2001, Niell et al., 2004). Imaging individual brain neurons expressing the fluorescently tagged postsynaptic marker PSD-95 supports a synaptotropic model of dendritogenesis in which synapse formation stabilizes filopodia, allowing further extension and branch formation (Vaughn et al., 1988, Niell et al., 2004, Chen et al., 2010). Therefore, contact with appropriate presynaptic terminals and activity-dependent synapse formation may direct dendritic branch formation and growth. Lacking from this model, however, is a comprehensive quantification of interstitial filopodial growth dynamics and their relationship to branch formation *in vivo*.

While growth cones on leading tips of axons have been extensively characterized for their roles in guidance and their morphological changes associated with axonal growth behaviors, reports on the existence of DGCs in intact brain tissues are scant (Vaughn et al., 1974, McMullen et al., 1988, Dailey and Smith, 1996, Tamamaki, 1999, Wu et al., 1999, Polleux et al., 2000, Furrer et al., 2003, Gascon et al., 2006). However, neurons typically orient their dendrites in a characteristic manner, and several axonal guidance cues, including Semaphorin 3A, Netrin-A and -B, and Slit, have been shown to direct orientation of dendritic growth (Polleux et al., 2000, Godenschwege et al., 2002, Furrer et al., 2003, Komiyama et al., 2007).

In order to further understand the roles of dendritic filopodia and DGCs in dendritogenesis within native environments, we have undertaken a comprehensive study of rapid dendritic arbor growth of newly differentiated projection neurons within the optic tectum of the intact and unanesthetized *X. laevis* tadpole. By tracking and measuring all dendritic processes in three dimensions from rapid and long-interval time-lapse imaging, we achieve sensitive measures of "dynamic morphometrics" that characterize the contributions of rapid growth behavior to the mature arbor structure. We find that all growing dendritic branches express DGCs, with morphologies correlating to distinct growth behaviors. Further we demonstrate that interstitial filopodia are precursors of longer and persistent dendritic branches.

METHODS

Animals

Freely swimming albino *X. laevis* tadpoles were housed at 22°C in 10% Steinberg's solution (1× Steinberg's: 10 m*M* HEPES, 60 m*M* NaCl, 0.67 m*M* KCl, 0.34 m*M* $(CaNO_3)_2$, 0.83 m*M* $MgSO_4$, pH 7.4) and maintained on a 12-h light/dark cycle. Experiments were conducted on Stage 47 tadpoles (Nieuwkoop and Faber, 1994), and were performed within guidelines set by the Canadian Council on Animal Care following protocols approved by the Animal Care Committee of the Faculty of Medicine at the University of British Columbia.

Single-Cell Electroporation

Individual projection neurons within the mediocaudal optic tectum of the intact tadpole brain were fluorescently labeled using single-cell electroporation (SCE) (Haas et al., 2001, Hewapathirane et al., 2008). Tadpoles were briefly anesthetized with 0.02% 3-aminobenzoic acid ethyl ester (MS222, Sigma). A sharp glass pipette (~0.6 μm tip diameter) loaded with a solution of plasmid DNA encoding farnesylated Green Fluorescent Protein (pEGFP-F, Clontech; 2 μg/μL in dH2O) was inserted into the proliferative zone in the mediocaudal region of the optic tectum, to transfect individual newly differentiated neurons using an Axoporator 800A (Molecular Devices, Sunnyvale, CA; stimulus parameters:

pulse intensity = 1 μA; pulse duration = 1 msec; pulse frequency = 300 Hz; train duration 300 msec).

In Vivo Time-Lapse Two-Photon Imaging in the Unanesthetized Brain

In order to image dynamic neuronal growth *in vivo* without the confounding effects of activity blockade from anesthetics, awake tadpoles were immobilized with the reversible paralytic pancuronium dibromide (PCD, 3 m*M*, Tocris) and mounted on a custom-built imaging chamber, embedded under a thin layer of agarose (1%) and continuously perfused with oxygenated 10% Steinberg's solution. Images of fluorescently labeled neurons were acquired using a custom-built two-photon microscope consisting of a modified Olympus FluoView 300V confocal scan box mounted on an Olympus BX50WI microscope coupled to a Chameleon Ti:Sapphire laser (Coherent, Santa Clara, CA). Three-dimensional stacks of images of the entire dendritic arbor were captured using a LUMPlanFI_IF 60×, 1.1 NA, water immersion objective (Olympus) and FluoView software (Olympus). Optical sections were acquired using 1.5 μm *z*-axis intervals, and stacks of images encompassing entire dendritic arbors were taken at 5 min intervals for 1 h each day for 5 consecutive days, at 5 min intervals for 5 h, or at 2 h intervals for 10 h. Following imaging, tadpoles were returned to rearing solution where they rapidly recovered from the paralytic.

Analysis of Dendritic Arbor Growth

Tectal neuron dendritic arbor morphology and growth were measured using custom written software to identify, track, and measure all dendritic branches and filopodia across all time points (software created by Dr. Jamie Boyd and Kaspar Podgorski, University of British Columbia). In all cases, all processes on the entire dendritic arbors were measured in three dimensions. Filopodia were defined as short, $<$10 μm, processes of uniform width and lacking protrusions. Due to differences in growth behaviors, including rates of addition, retraction, and lifetimes, filopodia were classified as either "interstitial," emerging from a dendritic shaft, or "branchtip," emerging within 5 μm of the branch ending. DGCs were defined as elaborations at the ends of processes, characterized by lamellipodial swellings with a width at least 1.5 times the width of the process shank, or the presence of a high density of filopodia over time. Filopodia and branch motility were measured by taking the sum of the absolute value of extensions and retractions over time. Proportions were analyzed using χ^2 tests followed by pair-wise *post hoc* comparisons (Chien et al., 1993), and Sholl analysis of branch length between successive spheres of increasing radii centered on the soma was conducted using two-way ANOVA followed by Bonferroni post tests. Differences in Day 1 to 2 *versus* Day 4 to 5 neurons and interstitial *versus* branchtip filopodial dynamics were analyzed using unpaired Student's *t*-tests. Multiple comparisons were done using one-way ANOVA followed by *post hoc* analysis by Tukey's multiple comparison test.

RESULTS

Tectal Neurons Progress through Three Phases of Dendritic Arbor Growth

As demonstrated previously (Wu et al., 1999, Haas et al., 2006, Liu et al., 2009), we find that *Xenopus* tectal neurons elaborate dendritic arbors over the course of 4 to 5 days after differentiation (see Fig. 1). Newly differentiated neurons first extend an axon without substantial dendritic branch formation or elongation over 24 h. As shown by Sholl analysis, the majority of dendritic arbor complexity is restricted proximal to the soma [Fig. 1(C)]. During this period, a high rate of dendritic filopodial turnover occurs without branch extension. Over the next 2 days, a growth spurt is driven by new branch addition and elongation. By the fourth day, dendritic arbor growth subsides and a stable state is reached with little net change in total dendritic branch length (TDBL), total dendritic branch number (TDBN), or three-dimensional arbor complexity [Fig. 1(B–D)]. These results are in accordance with previous characterization of three phases of vertebrate dendritogenesis (Wu et al., 1999). In Phase 1, newly differentiated neurons exhibit axonal growth with the dendritic arbor restricted to short and unstable protrusions. In Phase 2, over 24 to 48 h dramatic branch addition and elongation establishes the dendritic arbor. In Phase 3, this dramatic growth ceases and the dendritic arbor achieves a mature and stable conformation.

Dynamic Daily Imaging

To characterize dynamic dendritic growth behavior we employed rapid time-lapse imaging to capture the entire dendritic arbor every 5 min over 1 h. To measure growth behavior throughout distinct stages of maturation, dynamic imaging was conducted on the same neurons at 24 h intervals over 5 days. Importantly, all imaging was conducted on immobilized tadpoles without anesthesia, since neuronal transmission has been shown to regulate tectal dendrite growth (Rajan and Cline, 1998, Rajan et al., 1999, Sin et al., 2002, Haas et al., 2006, Ewald et al., 2008, Chen et al., 2010). Further, growth of all branches and filopodia on entire arbors were measured in three dimensions across all time points. We find that rapid time-lapse imaging reveals maturation-dependent dynamic growth behaviors undetectable from long-

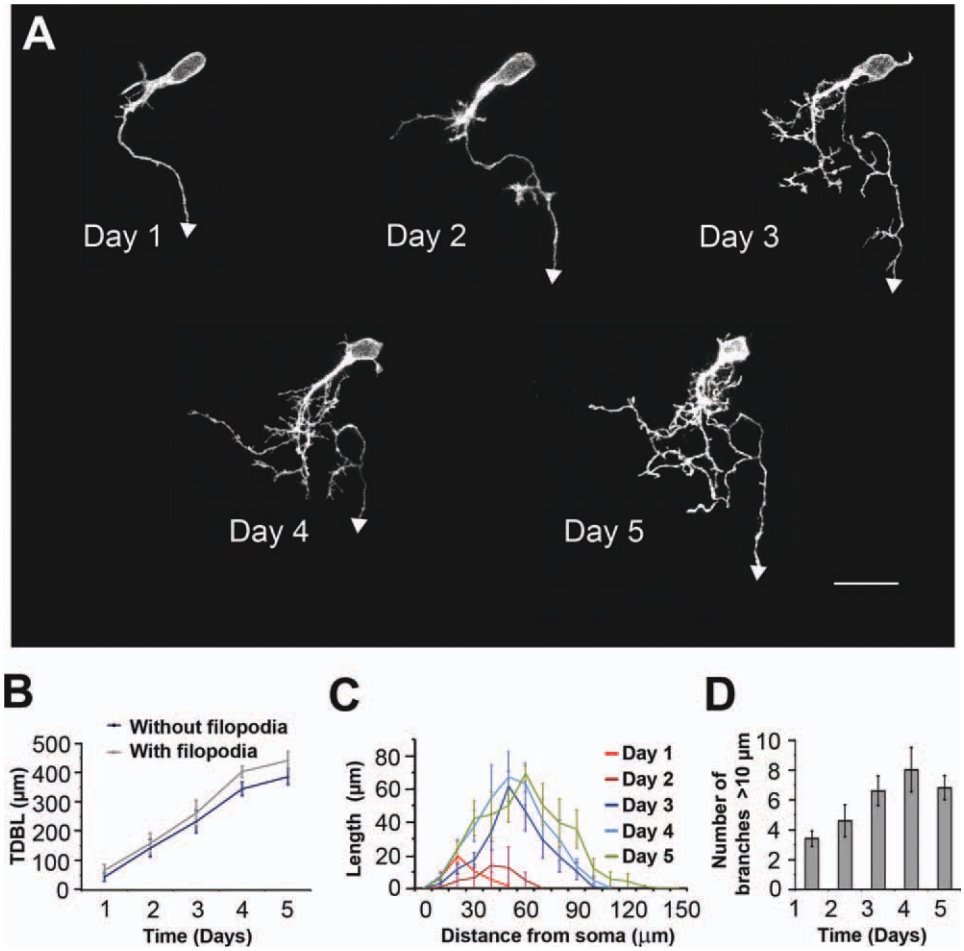

Figure 1 Maturation of tectal neurons *in vivo*. (A) Two-photon images of an individual neuron imaged at daily intervals for 5 days. The arrowhead depicts the axon, which projects out of the tectum. Scale bar = 20 μm. (B) Total dendritic branch length including and excluding all filopodia. (C) Three-dimensional Sholl analysis of changes in dendritic arbor complexity over 5 days. (D) Total number of dendritic branches >10 μm over 5 days. $N = 5$ neurons. Error bars denote SEM. [Color figure can be viewed in the online issue, which is available at wileyonlinelibrary.com.]

interval, "snap-shot" imaging (see Fig. 2). As shown in Figure 2(B), although DGCs are not visible at all time points, they are clearly visible from time-lapse imaging [see branchtips in over-lays, Fig. 2(B)]. Moreover, dendritogenesis involves a remarkable amount of turnover of filopodia and branches, transitions of filopodia into branches, and varied dendritic growth cone behaviors.

Dynamic Daily Imaging: Dendritic Branches

While we see little overall change in net dendrite growth over 1 h at any maturational state, dynamic growth behavior of dendritic branches changes over 5 days of neuronal development (see Fig. 2). Dendritic branches were characterized as processes >10 μm, or shorter processes exhibiting filopodial or branch protrusions, or any processes expressing lamellipodia. Branch motility significantly decreases over maturation, with 2.00 $\pm$ 0.12 μm/5 min on Day 1 to 2 to 1.22 $\pm$ 0.07 μm/5 min on Day 4 to 5 [all values presented as mean $\pm$ SEM; Fig. 2(C)]. Similarly, we find a maturational decrease in dynamic range, the difference between the longest and shortest length of each branch over 1 h [Fig. 2(E)], and a maturational increase in dendritic pausing behaviors as compared to extension and retraction behaviors which further corroborates evidence for increased dendritic stability with maturation [Fig. 2(F)]. Longer interval imaging, 2 h intervals over 10 h, was employed on Day 2 neurons to determine the lifetime of new branches [Fig. 4(C)]. Approximately half of new branches rapidly retracted within 2 h of initial detection, with 52.63%

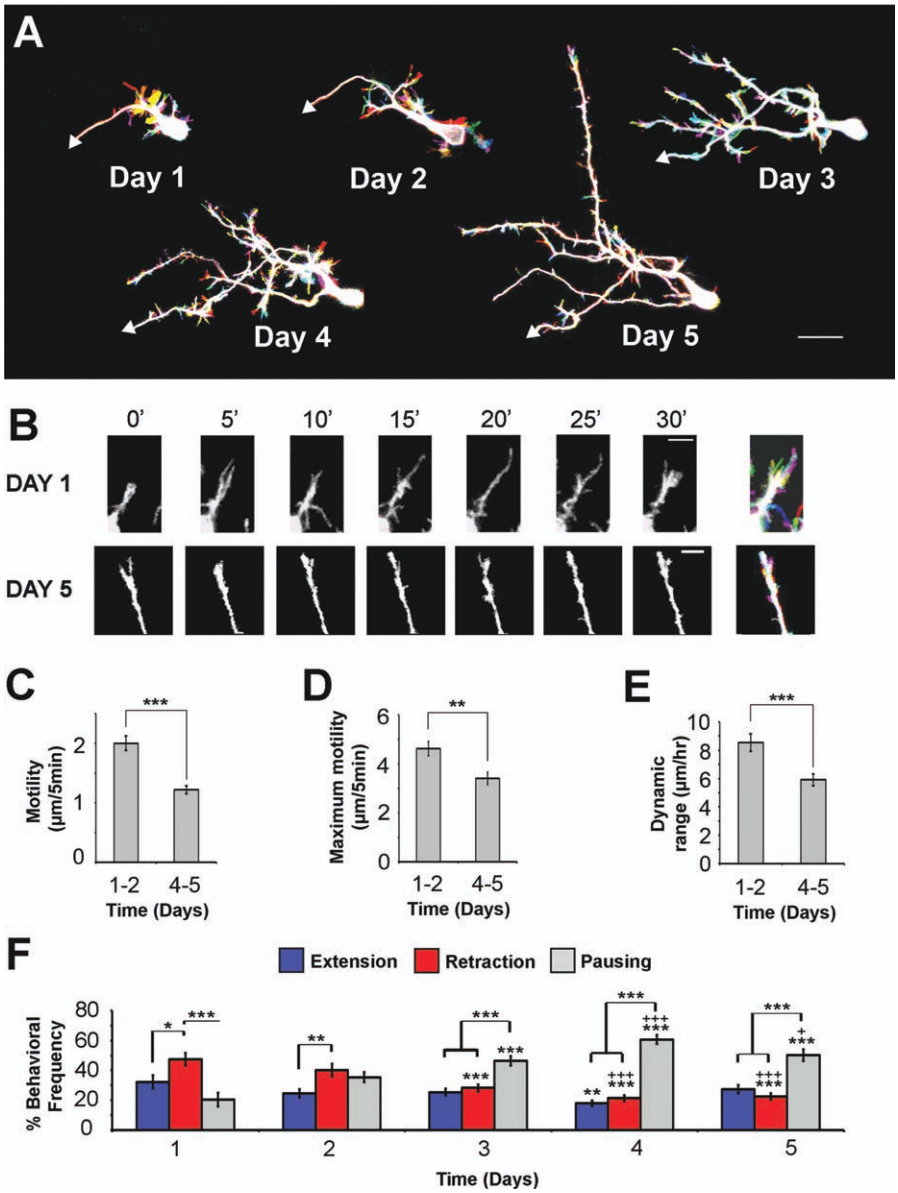

Figure 2 Maturation-dependent dynamic dendritic morphology and DGCs revealed by rapid time-lapse imaging. (A) Superimposed images of seven successive time points at 10 min intervals of a single neuron imaged daily for 5 days. Each time point within an overlay is a different color (red, green, blue, cyan, magenta, yellow, and orange; mixed colors and white = overlap). Arrowhead depicts the axon. Scale bar = 20 μm. (B) Images of a branchtip from a Day 1 neuron (top) and a Day 5 neuron (bottom) at 5 min intervals showing reduced motility and lamellipodia with maturation, followed by a superimposed image of all the time points in different colors (colors: red, green, blue, cyan, magenta, yellow, and orange; mixed colors and white = overlap; Scale bar = 5 μm). Note that for time point 20′ for the Day 1 neuron and 25′ for the Day 5 neuron the DGC is not discernible from a single image. (C) Motility, (D) maximum motility, defined as the maximum absolute value of extensions and retractions reached by each branch/5 min, and (E) dynamic range, defined as the absolute value of the maximum distance traveled by each branch/h, grouped by Day 1 to 2 neurons and Day 4 to 5 neurons (N = 5 neurons, n = 62 branches for Day 1–2 neurons and n = 82 branches for Day 4–5 neurons). (F) Percentage of the observed time points each branch undergoes extension, retraction, or pausing behaviors over 5 days of dynamic imaging. "*" denotes comparison with Day 1 and "+" denotes comparison with Day 2. Error bars denote SEM; *$p < 0.05$; **$p < 0.01$; ***$p < 0.001$.

persisting for >2 h, and only 10.53% persisting for >8 h. Thus, branches on developing neurons are labile and susceptible to a high degree of turnover during morphological refinement.

Dendritic Filopodia

Dendritic filopodia are short (<10 μm) and highly motile dendritic processes of uniform thin width expressed on branches throughout the growing dendritic arbor. Based on distinct growth behaviors, we have separated dendritic filopodia as "branchtip" if within 5 μm of a branch ending, and all others as "interstitial" (Portera-Cailliau et al., 2003). Branchtip filopodia typically exhibited shorter lifetimes, higher density, and higher addition and retraction rates compared with interstitial filopodia (see Fig. 3). Extrapolating from measures of filopodial addition rates from 5 min interval imaging over 1 h, every day for 5 days, we estimate that each tectal neuron produces approximately 3628 interstitial and 2402 branchtip filopodia over 5 days of dendritic arbor maturation. By imaging Day 2 neurons at 5 min intervals over 5 h and tracking every filopodia, we find that filopodia exhibited an average lifetime of 16.01 $\pm$ 1.89 min for interstitial and 10.57 $\pm$ 1.89 min for branchtip filopodia. Furthermore, we find a developmental shift in filopodial growth behavior. Immature Day 1 to 2 neurons exhibit higher filopodial motility and increased length as compared with more mature neurons [Fig. 3(E,F)]. Interstitial filopodia exhibit an increase in lifetime with maturation, with approximately 6.7 min for Day 1 neurons and 21.3 min for Day 5 neurons [Fig. 3(G)].

Dendritic Filopodia Emerging during Dendritogenesis are Precursors of Longer Branches

The function of dendritic filopodia has been an area of debate, which has largely focused on their relation to dendritic spines. Here, by tracking filopodia across 5 min intervals over 5 h, we find that interstitial dendritic filopodia can transition into branches during periods of arbor elaboration (see Fig. 4). Filopodia-to-branch transitions were defined as filopodia that extend to lengths greater than 10 μm, and/or elaborate lamellipodia at their endings, and/or extend additional processes. Of 1347 filopodia tracked across 5 min interval imaging over 5 h on complete arbors of 5 Day 2 neurons, 4.68% transformed into dendritic branches, and of these, 13.4% attained a length >10 μm. A breakdown of the three types of transitions reveal that most of these filopodia-to-branch transitions occurred by extending additional processes (48.48%) or by a combination of developing lamellipodia, branching, or attaining a length >10 μm over the 5 h imaging period [Fig. 4(D)]. While a low percentage (6.06%) of filopodia transitioned by developing only lamellipodia, none transitioned solely by increasing in length to >10 μm. From dynamic imaging over 5 days, we find that the percentage of filopodia that transition into branches decreases over neuronal maturation [Fig. 4(B)]. Although newly formed branches are unstable and exhibit a high rate of retraction, some nascent branches arising from interstitial filopodia were observed to persist for hours until the end of imaging [Fig. 4(C)]. The lifetime and average length of processes that underwent filopodia-to-branch transitions were significantly greater than for filopodia that did not transition to branches [Fig. 4(E,F)]. Therefore, during dendritogenesis, dendritic filopodia can function as precursors of longer and persistent branches, and expression of DGC appears to be a requirement for branch formation.

Dendritic Growth Cones (DGCs)

Rapid imaging reveals that dendritic endings exhibit dynamically changing morphologies with intermittent display of lamellipodia and/or a high density of branchtip filopodia, characteristics of growth cones [Fig. 2(A,B)]. A lamellipodium was defined morphologically as a dendritic ending with a width greater than 1.5 times the width of the adjacent dendritic shaft. In order to determine the expression pattern of DGCs throughout neuronal maturation and their relationship to dendritic growth, we examined all branch endings in all rapid time-lapse imaging experiments. Remarkably, given the paucity of published reports on DGCs, we find that all growing branches (>5 μm net growth/h) expressed DGCs identifiable by the presence of lamellipodia and/or a high density and turnover of branchtip filopodia [Fig. 6(C)]. DGCs are not readily apparent from single images because characteristic lamellipodia are observed in only 10% to 30% of images captured at 5 min intervals [Fig. 2(B)]. DGC morphology fluctuates dramatically within minutes from structures containing lamellipodia, both lamellipodia and filopodia, only filopodia, or none of these structures. The presence of DGCs on all growing branches suggests a central role in dendrite growth.

DGC Morphology Changes over Maturation

To determine whether DGC morphology changes over dendritic arbor maturation we examined mor-

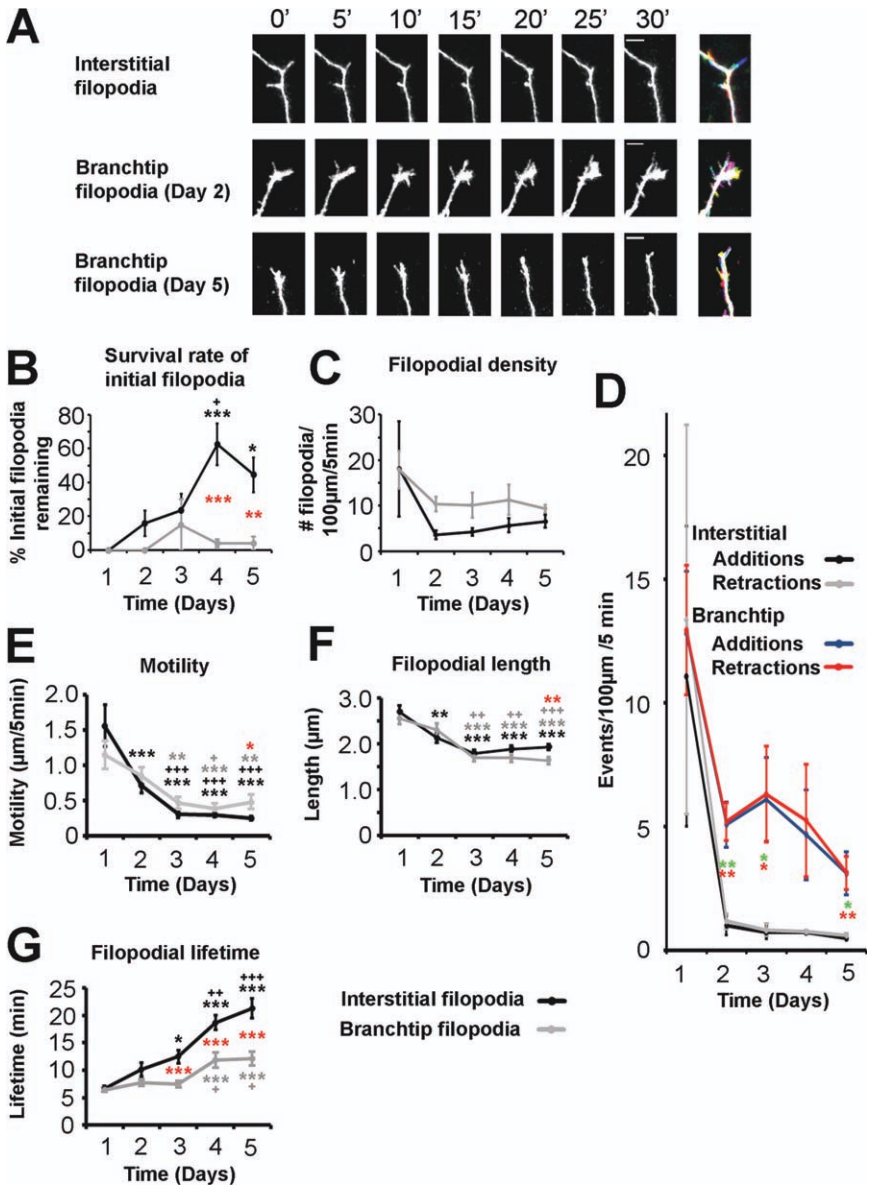

Figure 3 Comparison of branchtip and interstitial filopodial dynamics over neuronal maturation. (A) Rapid time-lapse images of interstitial filopodia from a Day 5 neuron (top), branchtip filopodia from a Day 2 neuron (middle), and branchtip filopodia from a Day 5 neuron (bottom), followed by an overlay of all time points shown (right) (colors used were red, green, blue, cyan, magenta, yellow, and orange; mixed colors and white = overlap; scale bars = 5 μm). (B) Percent of pre-existing branchtip and interstitial filopodia that survived until the end of the 1 h imaging period for Days 1 to 5. (C) Filopodial density, (D) additions and retractions, (E) motility, (F) length, and (G) lifetime for both branchtip and interstitial filopodia for Days 1 to 5. $N = 5$ neurons; $n = 26$, 30, 36, 48, and 44 branchtip filopodia and $n = 24$, 50, 85, 167, and 173 interstitial filopodia for Days 1 to 5, respectively. For significance on (B, E, F, and G), "*" denotes comparison with Day 1 and "+" denotes comparison with Day 2, gray for branchtip and black for interstitial filopodia. Red "*" denotes comparison between interstitial and branchtip filopodia. For (D), green and red "*" signify comparison of additions and retractions respectively between interstitial and branchtip filopodia. Error bars denote SEM; *, $+p < 0.05$; **, $++p < 0.01$; ***, $+++p < 0.001$.

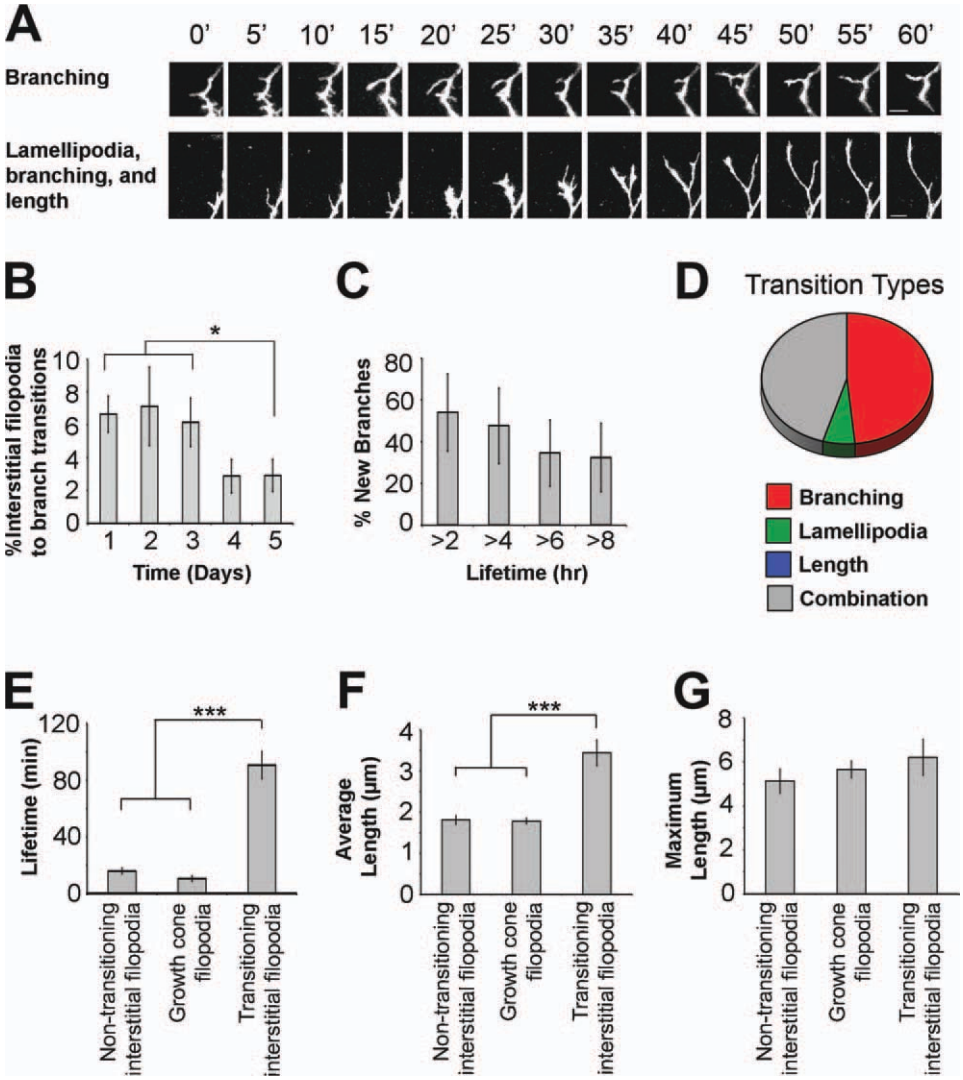

Figure 4 Interstitial filopodia transition to persistent dendritic branches. (A) Rapid time-lapse images of filopodia transitioning to a branch by branching (top, see t = 45 min), and by expressing lamellipodia, branching and increasing length to >10 μm (bottom). Scale bar = 5 μm. (B) Percent of interstitial filopodia that transition to branches within 1 h over Days 1 to 5. $N = 5$ neurons. (C) Lifetime of newly emerged branches obtained from imaging each neuron at 2 h intervals for 10 h. $N = 5$ neurons. (D) Percentage of each type of observed filopodia-to-branch transitions from imaging at 5 min intervals for 5 h. $N = 5$ neurons, $n = 66$ filopodia-to-branch transition events. (E) Lifetime, (F) average length, and (G) maximum length of "non-transitioning interstitial filopodia," "growth cone filopodia," and "transitioning interstitial filopodia" from imaging at 5 min intervals for 5 h. $N = 5$ neurons for (D–E). Error bars denote SEM; *, $+p < 0.05$; **, $++p < 0.01$; ***, $+++p < 0.001$. [Color figure can be viewed in the online issue, which is available at wileyonlinelibrary.com.]

phologies of all branch endings throughout 5 min/1 h dynamic imaging over 5 days of arbor growth. Branch endings were classified into categories based on presence or absence of lamellipodia or filopodia. Across all 5 days, the dominating branch morphologies were bare endings, or with only filopodia, with lower frequencies of expression of lamellipodia [Fig. 5(D)]. These results underscore the difficulty in identifying DGCs from single-image data. Maturational changes in DGC morphology were evident as a decrease in the expression of lamellipodia, which were significantly more prevalent on Day 1 to 2 neurons than Day 4 to 5 neurons [Fig. 5(D)]. In contrast, the frequency of

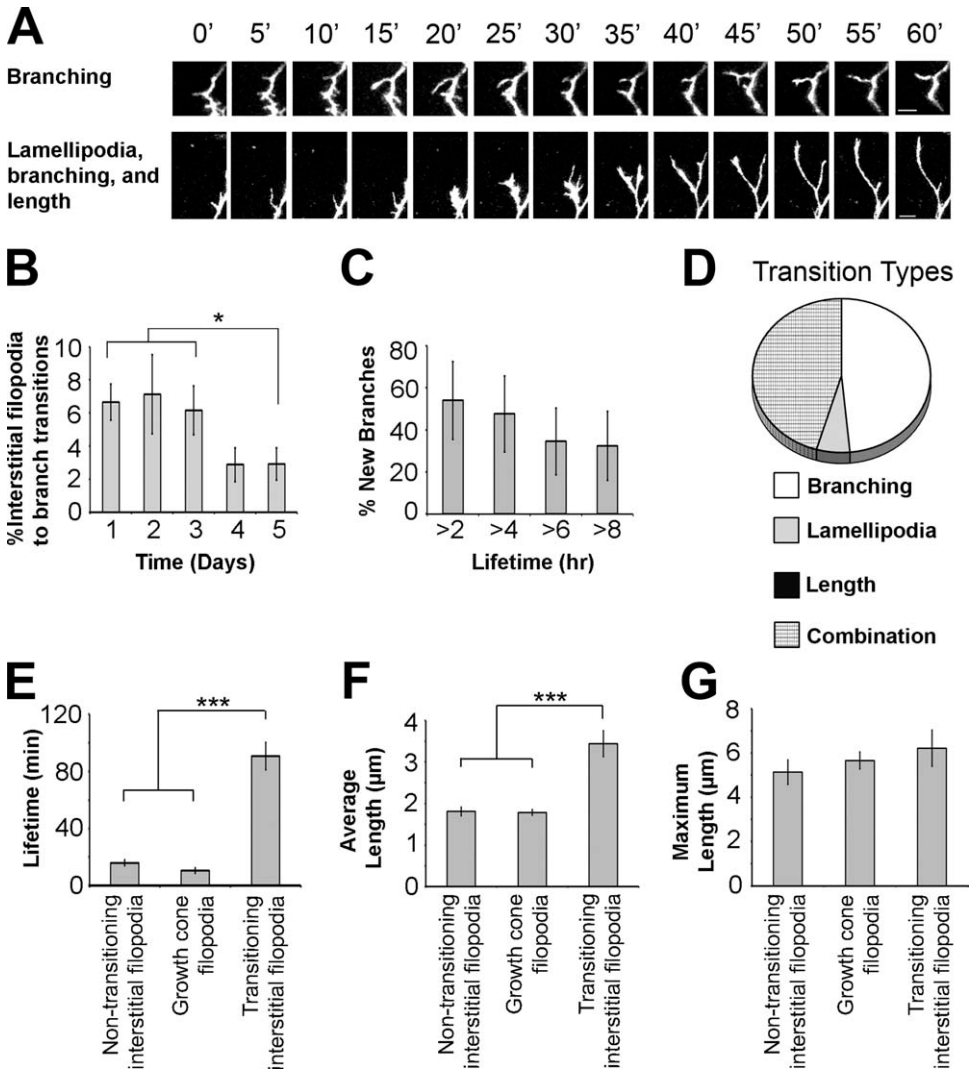

Figure 5 Morphological maturation of DGCs involves decrease in lamellipodia and increase in filopodia. DGC morphologies of the same set of five neurons were tracked over 5 days. (A) Images of three DGC exhibiting lamellipodia from Day 1 to 2 neurons (top) and from Day 4 to 5 neurons (bottom). Scale bar = 5 μm. (B) Maximum width of DGC lamellipodia over 5 days. $N = 5$ neurons, and $n = 18, 10, 13, 7, 11$ lamellipodia for Days 1, 2, 3, 4, and 5 respectively. (C) Percent of all branches with DGCs as indicated by the presence of lamellipodia or high filopodial density. $N = 5$ neurons. (D) Percentage of time points DGCs exhibited different morphologies for Days 1 to 2 neurons *versus* Day 4 to 5 neurons. "All Lamellipodia" includes DGC morphologies with lamellipodia alone or lamellipodia with filopodia. $N = 5$ neurons, and $n = 35$ DGCs for Days 1 to 2 and $n = 32$ DGCs for Days 4 to 5. Error bars denote SEM; $*p < 0.05$; $**p < 0.01$; $***p < 0.001$.

DGCs with only filopodia was lower for Day 1 to 2 neurons as compared with Day 4 to 5 neurons. Furthermore, the average lamellipodial width of DGCs was significantly reduced from 2.42 ± 0.22 μm on Day 1 to 1.6 ± 0.14 μm on Day 5 [Fig. 5(A,B)]. These results suggest a progression of DGC morphologies from lamellipodial to filopodial structures over neuronal maturation.

DGC Morphology Correlates with Extension, Retraction, and Pausing Behaviors

Given evidence for an association between axonal growth cone morphology with axonal growth behavior (Mason and Wang, 1997), we examined the relationship of DGC morphology to extension, retraction,

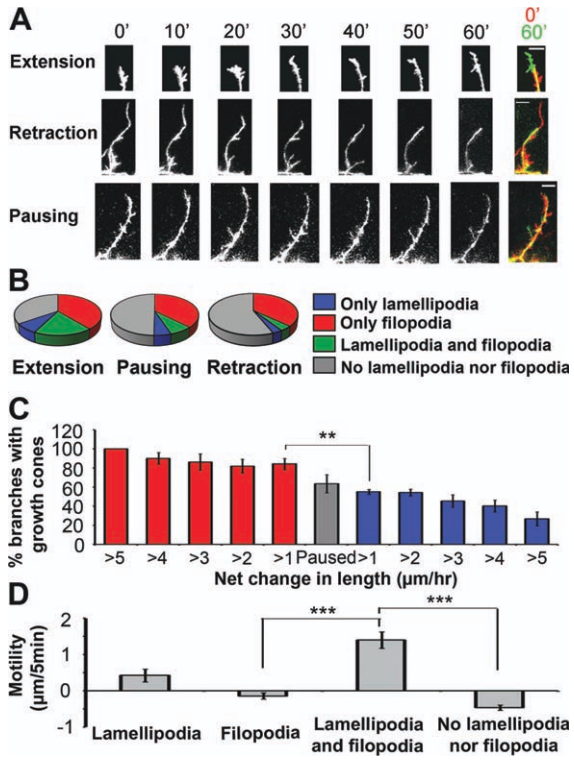

Figure 6 DGC morphology correlates with dendrite growth behavior. (A) Rapid time-lapse images of the branchtips of an extending dendrite from a Day 5 neuron (top), a retracting branch from a Day 2 neuron (middle), and a paused branch from a Day 4 neuron (bottom), shown at 10 min intervals, followed by an overlay of the first (red) and last (green) time points (right). Scale bar = 5 μm. (B) Percentage of each branch growth behavior, including extension, pausing, and retraction, exhibiting specific branchtip morphologies. (C) Dendrite growth over 1 h binned by the amount of net change in length and plotted with respect to the presence or absence of DGCs on each branch. Red bars denote extension, gray bars denote pausing, and blue bars denote retraction. $N = 5$ neurons. (D) Average branch motility for four different branchtip structures, including "lamellipodia," "filopodia," both "lamellipodia and filopodia," and "no lamellipodia nor filopodia." $N = 5$ neurons, $n = 85$, 621, 146, and 791 behaviors for "lamellipodia," "filopodia," "both lamellipodia and filopodia," and "no lamellipodia nor filopodia," respectively. Error bars denote SEM; *$p < 0.05$; **$p < 0.01$; ***$p < 0.001$.

and pausing behavior of dendrites. Axonal growth cones exhibit streamlined morphologies during periods of rapid growth and more complex lamellipodial morphologies while pausing. We find that all branches exhibiting greater than 5 μm/h net extension expressed DGCs [Fig. 6(A,C)]. Of all the paused dendritic branches, defined as exhibiting less than 1 μm/h net change in length, 63.4 $\pm$ 9.4% expressed DGCs, while only 26.7 $\pm$ 7.3% of retracting branches (greater than 5 μm/h net retraction) expressed DGCs [Fig. 6(C)]. Furthermore, binning net branch extension and retraction by 1 μm/h intervals shows a clear trend of increasing percent of branches with growth cones with increasing net extension and a decreasing presentation of growth cones with increasing net retraction. To analyze this relationship between branch morphology and behavior in more detail, we compared DGC morphology immediately before the branch growth behavior for each 5 min interval of rapid time-lapse imaging. For this analysis, over each 5 min interval, greater than 1 μm of branch elongation was defined as "extension," greater than 1 μm of branch shortening as "retraction," and <1 μm movement as "pausing." We find that lamellipodia are associated with extensions (26.12%) and to a lesser extent pausing, and not retractions [6.88%; Fig. 6(B)]. In contrast, morphologies lacking lamellipodia and filopodia are associated to a larger extent with retractions (56.13%) then extensions (34.83%). Furthermore, average motility of branches expressing both lamellipodia and filopodia (1.40 $\pm$ 0.22 μm/5 min) were significantly greater than the average motility of branches without lamellipodia or filopodia (-0.46 ± 0.07 μm/5 min). These results indicate that growth cones on dendrites of developing brain neurons are associated with both pausing and active extension, whereas retracting dendrites tend to express a collapsed morphology.

DISCUSSION

Using a combination of short- and long-interval time-lapse imaging of growing dendrites in the intact and unanesthetized developing brain, we address fundamental questions regarding the function and behaviors of key components of the developing dendritic arbor, including dendritic filopodia and growth cones. By employing powerful custom-built software to track and measure all processes on entire dendritic arbors in three dimensions over short intervals for long periods, we characterize the contributions of these structures to neuronal morphological maturation. This comprehensive quantification and novel analysis offers unprecedented detail of dynamic growth behaviors and their changes across different stages of dendritic arbor development.

Our identification of DGCs at the ends of all extending branches is in contrast to the limited description and study of these complex cellular specializations in published literature (Vaughn et al.,

1974, McMullen et al., 1988, Dailey and Smith, 1996, Tamamaki, 1999, Wu et al., 1999, Polleux et al., 2000, Furrer et al., 2003, Gascon et al., 2006). Lack of attention to DGCs *in vivo* is most likely due to technical limitations in conducting rapid time-lapse imaging of dendrite development. Our results demonstrate that since DGCs typically exhibit temporally varying and relatively small lamellipodia compared with axonal growth cones, these structures are often not apparent in single time point images. Also, we find that although DGCs are associated with a higher density of branchtip filopodia over time than at interstitial regions, this difference is most evident from examining multiple time points.

Previous studies have described two major categories of axonal growth cone functions: facilitating process elongation and providing orientation (reviewed in Lowery and Van Vactor, 2009). However, the relevance of DGCs *in vivo*, and specifically to what extent they share functions with their axonal counterparts remain largely unexplored. Previous studies in fixed tissue and in acute slices provide evidence supporting DGC involvement in both dendritic orientation (Polleux et al., 2000, Godenschwege et al., 2002, Furrer et al., 2003, Komiyama et al., 2007) and extension mediated by increased microtubule stabilization (Gascon et al., 2006). Our findings suggest DGCs are essential for dendritic growth *in vivo* in the developing central nervous system since they occur on all actively extending branches, and are rapidly expressed by filopodia transitioning into branches. Axonal growth cone morphology correlates with extension and pausing behaviors, such that in rapid growth phases, axonal growth cones exhibit streamlined appearance, while during pausing at choice points, they exhibit broad fan-like lamellipodia and filopodia (Bovolenta and Mason, 1987, Mason and Wang, 1997, Mason and Erskine, 2000). In contrast, we find that lamellipodia on DGCs are relatively small and are primarily expressed on extending branches, and to a lesser extent on pausing branches. Dendritic growth occurs by intermittent extension, retraction, and pausing behaviors within minutes, which over a longer period results in slow net rate of elongation of approximately 5 μm/h. In contrast, extending axons advance with a consistent and much higher growth rate of approximately 55 μm/h (Mason and Erskine, 2000). The display of lamellipodia during pausing behavior in axons, yet during both extension and pausing behaviors in dendrites may reflect distinct growth patterns corresponding to requirements for axons to extend across long distances through uniform tissue, while dendrites need to orient across shorter domains while also forming and testing synapses.

This study is the first to characterize developmental changes in DGC morphology *in vivo*. We find that as neurons mature, DGC morphology shifts to reduce the size and frequency of lamellipodia, and to increase the frequency of branchtip filopodia. Lamellipodia are largest at initial stages of primary branch extension, potentially suggesting a critical decision point to detect external cues for initial orientation of branch growth. Further, lamellipodia have been shown to be necessary for stabilization of new branches in immature neurons (Gascon et al., 2006). At stages when activity-dependent CaMKII-mediated synaptogenesis is not available to promote dendritic stabilization (Wu and Cline, 1998, Zou and Cline, 1999), lamellipodia may play an important role to prevent process retraction. As branches elongate and mature, lamellipodia become smaller and less frequent, and branch endings shift to expression of highly dynamic filopodia. This transition may be due to branches reaching appropriate termination zones within neuropil, and an altered role from orientation to identification of synaptic contacts.

We find that interstitial dendritic filopodia are precursors of longer and more persistent branches. Our results demonstrate there are distinct classes of dendritic filopodia on immature neurons during dendritogenesis that give rise to dendrites or are associated with DGCs. The origin of new dendritic branches has been debated, with lamellipodial splitting reported to be the dominant mechanism of dendritic branching in cultured neurons (Bray, 1973, Scott and Luo, 2001). In contrast, filopodia transitioning to branches has been demonstrated in brain slices and *in vivo* (Dailey and Smith, 1996, Niell et al., 2004). The low rate of filopodial transitions to branches we observed here suggests a high threshold for morphological stabilization, likely induced by synapse formation (Vaughn et al., 1988, Niell et al., 2004, Chen et al., 2010). However, given the relatively small number of branches comprising the mature and stable arbor, each transition event leading to a persistent branch contributes significantly to the computational capabilities of the neuron on which it resides.

This study of developing projection neurons within Stage 47 *Xenopus* tadpoles examines dendritic growth into a functional visual circuit undergoing activity-dependent refinement. Relevance of these finding to other vertebrate systems is supported by observations of dendritic growth cone guidance (Polleux et al., 2000) and activity-dependent dendritogenesis in rodent cortex (Espinosa et al., 2009). Our results employing rapid and long interval time-lapse imaging and comprehensive morphological quantification reveal multiple mechanisms of directed dendritic arbor growth

including maturation dependent expression of DGCs potentially providing orientation, and high interstitial filopodial and branch turnover suggesting extensive sampling of local environments for appropriate presynaptic contacts. Together, these growth programs allow external cues and intercellular interactions to contribute to dendritic arbor patterning.

REFERENCES

Bovolenta P, Mason C. 1987. Growth cone morphology varies with position in the developing mouse visual pathway from retina to first targets. J Neurosci 7:1447–1460.

Bray D. 1973. Branching patterns of individual sympathetic neurons in culture. J Cell Biol 56:702–712.

Chen SX, Tari PK, She K, Haas K. 2010. Neurexin-neuroligin cell adhesion complexes contribute to synaptotropic dendritogenesis via growth stabilization mechanisms in vivo. Neuron 67:967–983.

Chien CB, Rosenthal DE, Harris WA, Holt CE. 1993. Navigational errors made by growth cones without filopodia in the embryonic Xenopus brain. Neuron 11:237–251.

Cline H, Haas K. 2008. The regulation of dendritic arbor development and plasticity by glutamatergic synaptic input: A review of the synaptotrophic hypothesis. J Physiol 586:1509–1517.

Dailey ME, Smith SJ. 1996. The dynamics of dendritic structure in developing hippocampal slices. J Neurosci 16:2983–2994.

Espinosa JS, Wheeler DG, Tsien RW, Luo L. 2009. Uncoupling dendrite growth and patterning: Single-cell knockout analysis of NMDA receptor 2B. Neuron 62:205–17.

Ewald RC, Van Keuren-Jensen KR, Aizenman CD, Cline HT. 2008. Roles of NR2A and NR2B in the development of dendritic arbor morphology in vivo. J Neurosci 28:850–861.

Furrer MP, Kim S, Wolf B, Chiba A. 2003. Robo and Frazzled/DCC mediate dendritic guidance at the CNS midline. Nat Neurosci 6:223–230.

Gascon E, Dayer AG, Sauvain MO, Potter G, Jenny B, De Roo M, Zgraggen E, Demaurex N, Muller D, Kiss JZ. 2006. GABA regulates dendritic growth by stabilizing lamellipodia in newly generated interneurons of the olfactory bulb. J Neurosci 26:12956–12966.

Godenschwege TA, Simpson JH, Shan X, Bashaw GJ, Goodman CS, Murphey RK. 2002. Ectopic expression in the giant fiber system of Drosophila reveals distinct roles for roundabout (Robo. Robo2, and Robo3) in dendritic guidance and synaptic connectivity. J Neurosci 22:3117–3129.

Grueber WB, Jan LY, Jan YN. 2003. Different levels of the homeodomain protein cut regulate distinct dendrite branching patterns of Drosophila multidendritic neurons. Cell 112:805–818.

Haas K, Li J, Cline HT. 2006. AMPA receptors regulate experience-dependent dendritic arbor growth in vivo. Proc Natl Acad Sci USA 103:12127–12131.

Haas K, Sin WC, Javaherian A, Li Z, Cline HT. 2001. Single-cell electroporation for gene transfer in vivo. Neuron 29:583–591.

Hausser M, Spruston N, Stuart GJ. 2000. Diversity and dynamics of dendritic signaling. Science 290:739–744.

Hewapathirane DS, Haas K. 2008. Single-cell electroporation *in vivo*. JoVE 17:705.

Jan YN, Jan LY. 2010. Branching out: Mechanisms of dendritic arborization. Nat Rev Neurosci 11:316–328.

Jinushi-Nakao S, Arvind R, Amikura R, Kinameri E, Liu AW, Moore AW. 2007. Knot/Collier and cut control different aspects of dendrite cytoskeleton and synergize to define final arbor shape. Neuron 56:963–978.

Komiyama T, Sweeney LB, Schuldiner O, Garcia KC, Luo L. 2007. Graded expression of semaphorin-1a cell-autonomously directs dendritic targeting of olfactory projection neurons. Cell 128:399–410.

Liu XF, Tari PK, Haas K. 2009. PKM zeta restricts dendritic arbor growth by filopodial and branch stabilization within the intact and awake developing brain. J Neurosci 29:12229–12235.

Lowery LA, Van Vactor D. 2009. The trip of the tip: Understanding the growth cone machinery. Nat Rev Mol Cell Biol 10:332–343.

Mason C, Erskine L. 2000. Growth cone form, behavior, and interactions in vivo: Retinal axon pathfinding as a model. J Neurobiol 44:260–270.

Mason CA, Wang LC. 1997. Growth cone form is behavior-specific and, consequently, position-specific along the retinal axon pathway. J Neurosci 17:1086–1100.

McAllister AK, Katz LC, Lo DC. 1997. Opposing roles for endogenous BDNF and NT-3 in regulating cortical dendritic growth. Neuron 18:767–778.

McMullen NT, Goldberger B, Glaser EM. 1988. Postnatal development of lamina III/IV nonpyramidal neurons in rabbit auditory cortex: Quantitative and spatial analyses of Golgi-impregnated material. J Comp Neurol 278:139–155.

Mumm JS, Williams PR, Godinho L, Koerber A, Pittman AJ, Roeser T, Chien CB, Baier H, Wong RO. 2006. In vivo imaging reveals dendritic targeting of laminated afferents by zebrafish retinal ganglion cells. Neuron 52:609–621.

Nedivi E, Wu GY, Cline HT. 1998. Promotion of dendritic growth by CPG15, an activity-induced signaling molecule. Science 281:1863–1866.

Niell CM, Meyer MP, Smith SJ. 2004. In vivo imaging of synapse formation on a growing dendritic arbor. Nat Neurosci 7:254–260.

Polleux F, Morrow T, Ghosh A. 2000. Semaphorin 3A is a chemoattractant for cortical apical dendrites. Nature 404:567–573.

Portera-Cailliau C, Pan DT, Yuste R. 2003. Activity-regulated dynamic behavior of early dendritic protrusions: Evidence for different types of dendritic filopodia. J Neurosci 23:7129–7142.

Rajan I, Cline HT. 1998. Glutamate receptor activity is required for normal development of tectal cell dendrites in vivo. J Neurosci 18:7836–7846.

Rajan I, Witte S, Cline HT. 1999. NMDA receptor activity stabilizes presynaptic retinotectal axons and postsynaptic optic tectal cell dendrites in vivo. J Neurobiol 38:357–368.

Scott EK, Luo L. 2001. How do dendrites take their shape? Nat Neurosci 4:359–365.

Sin WC, Haas K, Ruthazer ES, Cline HT. 2002. Dendrite growth increased by visual activity requires NMDA receptor and Rho GTPases. Nature 419:475–480.

Tamamaki N. 1999. Development of afferent fiber lamination in the infrapyramidal blade of the rat dentate gyrus. J Comp Neurol 411:257–266.

Vaughn JE, Barber RP, Sims TJ. 1988. Dendritic development and preferential growth into synaptogenic fields: A quantitative study of Golgi-impregnated spinal motor neurons. Synapse 2:69–78.

Vaughn JE, Henrikson CK, Grieshaber JA. 1974. A quantitative study of synapses on motor neuron dendritic growth cones in developing mouse spinal cord. J Cell Biol 60:664–672.

Wu GY, Cline HT. 1998. Stabilization of dendritic arbor structure in vivo by CaMKII. Science 279:222–226.

Wu GY, Zou DJ, Rajan I, Cline H. 1999. Dendritic dynamics in vivo change during neuronal maturation. J Neurosci 19:4472–4483.

Zou DJ, Cline HT. 1999. Postsynaptic calcium/calmodulin-dependent protein kinase II is required to limit elaboration of presynaptic and postsynaptic neuronal arbors. J Neurosci 19:8909–8918.